Scientia Iranica, Vol. 6, No. 2, pp 143–148

SCIENTIA
IRANICA

A New Approach in Modeling of Metal-Mold Interface in Casting Using Finite Element Method

M.T. Ahmadian*, M. Shirinparvar[1] and P. Davami[1]

In casting simulation, metal-mold interface consideration plays an important role in the accuracy of the results. In this paper, casting process is analyzed using Finite Element Method (FEM). An element with zero thickness is introduced for the interface of the metal and mold. Through this imaginary element, contact resistance and air gap at the interface are implemented. In FEM formulation, the convective heat transfer equation is considered to be governing the interface. Heat transfer coefficient of the interface is measured experimentally for casting of Al-12%Si in a cylindrical cast iron mold. Results of the simulation were satisfactory and in good agreement with experimental data.

INTRODUCTION

In a casting process, cast and mold do not have a complete contact due to surface tension, surface oxidation and mold roughness, and a contact resistance exists at the interface. Reduction of surface roughness, oxidation prevention and increasing metallostatic pressure will decrease this resistance.

As the cooling process begins, a solid skin develops. Due to contraction of the solid cast and expansion of the heated mold, an air gap will be formed at the interface. As a result of this gap, the mechanism of heat transfer at the interface becomes pure convection.

To predict the conduction of a casting process accurately, it is necessary to consider the effect of air gap and contact resistance in the simulation. Samonds et al. [1] and Tadayon et al. [2] have used a thin element model and coincident nodes techniques based on FEM to analyze the interface problem. However, in the thin element model, size of the air gap and its variation during the process of solidification must be known. Also, due to the large aspect ratio of the thin element, error will increase drastically. Moreover, in coincident nodes techniques, element properties are not satisfied and, consequently, physics of the problem will be changed.

An advanced solidification software must be capable of considering metallurgical microstructure, predicting porosity, contraction of melt, rate of solidification front and so on. Contact resistance and air gap are the fundamental factors in solidification rate and their effects on castings are substantial. A 10-second delay in the formation of air gap causes ten percent decrease in solidification time and a 50 percent increase in air gap thickness will result in a ten percent increase in solidification time [3]. This means that considering contact resistance and air gap is very essential in predicting solidification process correctly.

HEAT TRANSFER ANALYSIS AT METAL-MOLD INTERFACE

Heat transfer at metal-mold interface is very much dependent on the type of surface contact and the media in between. Surface contact of the metal-mold interface may be treated in one of the following ways (Figure 1):

1. Without contact resistance; ideal case.
2. With contact resistance.
3. Contact with a thin layer of gas as the media (air, moisture, gases due to burning of organic materials, the combination of them); air gap.

*. *Corresponding Author, Department of Mechanical Engineering, Sharif University of Technology, P.O. Box 11365-9765, Tehran, I.R. Iran.*

1. *Department of Metallurgical Engineering, Sharif University of Technology, P.O. Box 11365-9466, Tehran, I.R. Iran.*

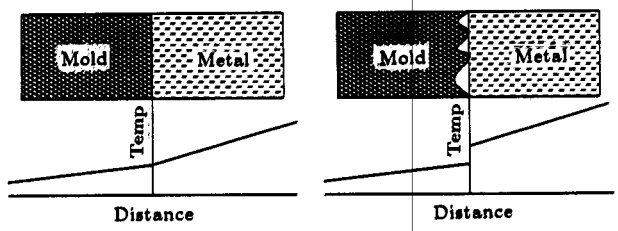

Figure 1. Schematic diagram of metal-mold interface and temperature distribution. a) Perfect contact; b)imperfect contact.

Complete contact can theoretically happen when surfaces are under high contact pressure and highly finished. Contact with resistance occurs when surfaces are not in complete contact which is usually due to roughness or coating of the mold and low pressure of the cast. This resistance exists until a thick solid skin is formed. In this case, heat is transferred through scattered contact points and gas spaces. Air gap occurs when solid skin is not deformed under metalostatic or external pressure. Due to contraction of the formed metal skin and expansion of the surrounding model surface, heat is transferred mostly through the layer of gas at the interface.

In general, heat is transferred through air gap at interface by means of convection, radiation and gas conduction. Figure 2 demonstrates the state of heat transfer condition in a system [4]. The values of Nuselt (Nu), Grashof (Gr) and Prandle (Pr) numbers are represented by the following equations:

$$Gr_d = \frac{g\beta(T_c - T_m)d^3}{\nu^2}, \tag{1}$$

$$Nu_d = \frac{hd}{K_g}, \tag{2}$$

$$Pr = \frac{C_P\mu}{K}. \tag{3}$$

Figure 2 and Equations 1 to 3 and casting conditions (gas pressure, depth of roughness and air gap thickness)

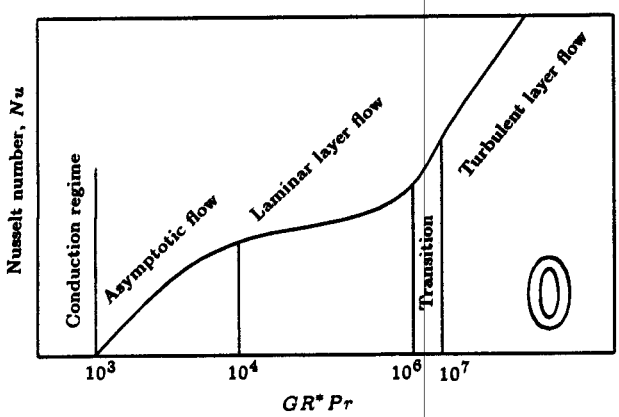

Figure 2. Schematic diagram and flow regimes of the vertical convection layer.

illustrate that a high percentage of heat transfer occurs via gas conduction and radiation, therefore, convection can be ignored in this process. It is also possible to define the temperature profile of the metal-mold interface using Knudsen number (Kn). The small value of the mean free path (λ) compared with the size of air gap (d), confirms that the temperature profile at the interface of casting can always be assumed linear and continuous [5].

$$Kn = \frac{\lambda}{d} \tag{4}$$

However, Fourier's law of heat transfer can be used at the interface. To calculate the overall heat transfer coefficient at the interface, it can be assumed that the media of the interface is a layer of gas (d). Now, the equivalent heat transfer coefficient is defined as:

$$h = \frac{k}{d}, \tag{5}$$

and:

$$h = \frac{\dot{q}}{A(T_c - T_m)}. \tag{6}$$

To predict the position of metal-melt interface and the rate of solidification, a fixed value of h can be considered; however, it is clear that this assumption is not accurate enough and the value of h varies with time and metallurgical parameters. Figure 3 represents variations of h with time for a typical casting process [6]. It is observed that heat transfer coefficient

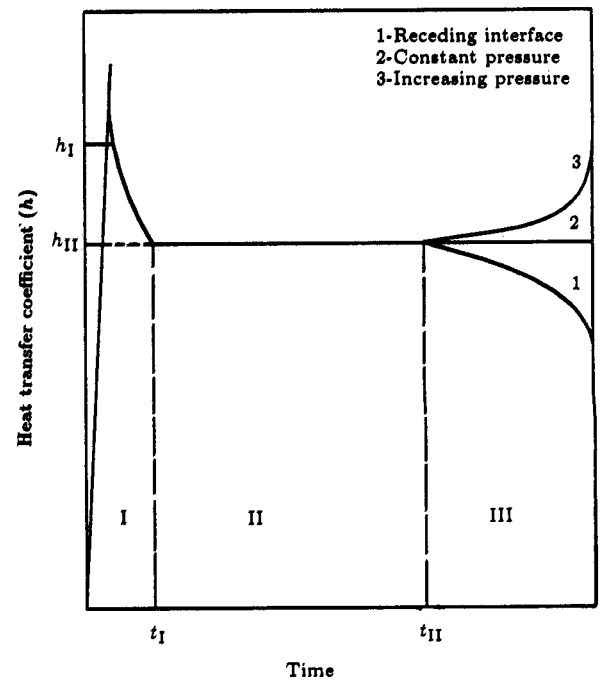

Figure 3. Schematic diagram of the h with time.

suddenly increases as the process of pouring the melt begins. As melt motion decreases, the heat transfer coefficient also decreases and gradually reaches a fixed value and remains constant until a solid skin is formed. After this stage, depending on the geometry of the mold and cast three possibilities may occur as shown in Figure 3.

1. Decrease in heat transfer coefficient due to formation of air gap.
2. Increase in heat transfer coefficient due to expansion of the core and contraction of the cast.
3. Heat transfer coefficient remains constant; this happens usually at the bottom of the metal-mold interface.

GOVERNING EQUATION

The heat transfer equation may be written as:

$$\rho C_P \frac{\partial T}{\partial t} = \nabla(k \nabla T). \tag{7}$$

To implement this equation, the following assumptions are made:

1. Temperature of the cast and mold are assumed to be uniform and equal to the pouring temperature and environment or preheat temperature, respectively.
2. Convection and melt movement, due to temperature variation during solidification, are ignored.
3. Melt shrinkage, due to temperature reduction in the process of solidification, is ignored.
4. Physical properties of the cast and mold are assumed always to be constant in the process of solidification.
5. Heat transfer in the mold, melt and solid skin take places only by means of conduction.
6. Latent heat of solidification is assumed to be uniform and constant.
7. Resistance at interface between solidification front and melt is ignored.
8. In the overall heat transfer coefficient calculation at the interface, the effect of conduction due to contact points, gas gap and radiation are considered.

Considering physical domain of Ω with boundaries of Γ_1 and Γ_2, the boundary condition may be written as (Figure 4):

$$T(r,t) = \hat{T}(r,t) \text{ at } \Gamma_1 \text{ Dirichlet B.C.},$$

and:

$$K \nabla T \cdot \hat{n} + q + h(T - T_a) = 0 \text{ at } \Gamma_2 \text{ Neuman B.C.}$$

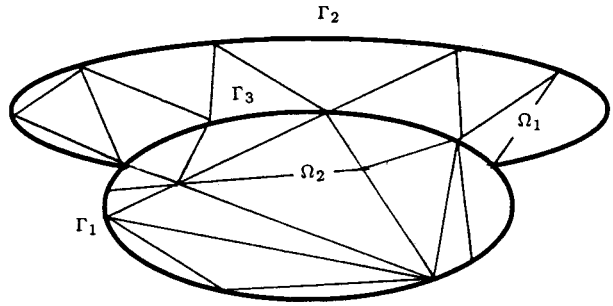

Figure 4. Physical domain and its boundary.

The initial condition for the problem is assumed to be:

$$T(r,0) = T_a \quad \text{in the mold},$$

$$T(r,0) = T_{\text{pour}} \quad \text{in the cast}.$$

FEM MODELING

Due to the symmetrical properties of the cylindrical geometry, the 3-D heat transfer equation reduces to a 2-D equation where through implementation, the FEM formulation may be written as [7-9]:

$$[C]\{\dot{T}\} + [K]\{T\} = \{F\}. \tag{8}$$

Stiffness matrix K, capacitance matrix C and force vector F are defined, respectively, as:

$$K_{ij} = \int_{\Omega} \nabla N_j (K \nabla N_j) d\Omega + \int_{\Gamma 2} h_b N_i N_j d\Gamma_2, \tag{9}$$

$$C_{ij} = \int_{\Omega} \rho C_P N_i N_j d\Omega, \tag{10}$$

$$F_i = -\int_{\Gamma a} (q - h_b T_a) N_i d\Gamma_2, \tag{11}$$

where T is the nodal temperature vector. It is important to note that the heat transfer at the central line of the cylinder has been neglected and convection takes place between the cylinder and the surrounding. In this work, the overall heat transfer coefficient has been measured experimentally, which includes the effect of conduction, convection, radiation and contact points.

To solve the transient part of Equation 7, the FDM technique is used, using the so-called Θ-method via the time stepping algorithms:

$$[C + \Theta K \Delta\tau]\{C\}_{i+1} = [C - (1 - \Theta)K\Delta\tau]\{C\}_i + [(1 - \Theta)F_i + \Theta F_{i+1}]\Delta\tau. \tag{12}$$

This method includes forward, central and backward difference schemes with values of $\Theta = 0$, 0.5 and 1, respectively [9].

MODELING OF ZERO THICKNESS ELEMENT AT INTERFACE

In the casting simulation problem, correct modeling of the mold-cast interface plays an important role in the accuracy of the results. Ignoring the interface in metallic mold results in an error between 50-100% in the solidification time. Most of the researchers have not considered air gap or contact resistance in their simulation and assumed the neighboring elements of cast and mold to be in full contact.

In this simulation, a Zero Thickness Element (ZTE) is introduced for implementation of the contact resistance and air gap [10]. Figure 5 represents such a model at an interface; nodes 3, 4, 5 and 6 are ZTE nodes, connecting elements A and B at cast and mold, respectively. Table 1 shows the node numbers configuration of the ZTE with the neighboring elements.

Heat is transferred at the interface between elements A and B by convection with an equivalent heat transfer coefficient, h, through ZTE. The shape function for ZTE considering local coordinate system of ξ and η may be written as:

$$N_1^{ZTE} = \frac{1}{2}(1-\xi),$$

$$N_2^{ZTE} = \frac{1}{2}(1+\xi). \tag{13}$$

The stiffness matrix for this element is defined as:

$$K_{ij}^e = \int_{\Gamma_3} hN_jN_i d\Gamma_3, \tag{14}$$

where Γ_3 represents the metal-mold boundary and h is the overall heat transfer at the interface. The overall heat transfer coefficient may be defined experimentally or calculated mathematically. Finally, Equation 13 may be written as:

$$K_{ij}^e = \int_{-1}^{1} hN_jN_i|J|nd\xi, \tag{15}$$

where n is the unit normal to the surface of the integration and should be selected properly based on the physics of the problem.

Table 1. Node numbers configuration of the ZTE with the neighboring elements.

Elements	Number of Nodes			
A	3	4	2	1
ZTE	5	6	4	3
B	7	8	6	5

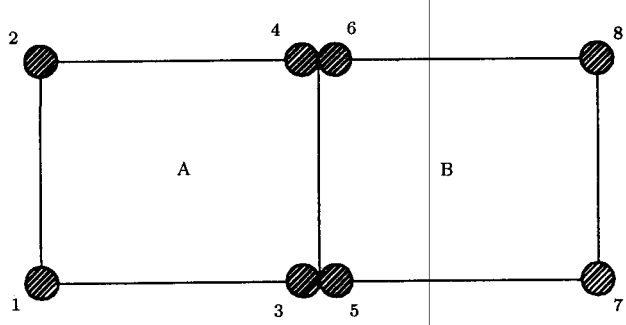

Figure 5. Zero thickness element at interface.

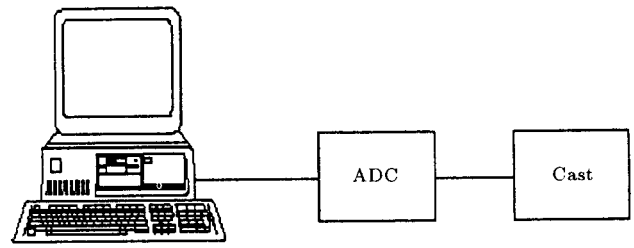

Figure 6. Experimental set-up.

EXPERIMENTAL SET-UP

To measure the overall heat transfer coefficient, h, an experiment was designed (Figure 6) in which the mold was a gray iron cylinder with isolated top and bottom. In this experiment, seven (Ni, Ni-Cr) thermocouples, an eight-channel 12 bit A/D converter and a 486-DX computer have been used. Data were stored every 300 milliseconds for 15 minutes (Complete solidification occurs after 70 sec).

The overall heat transfer coefficient at the interface, measured experimentally, versus time is represented in Figure 7. It is clear that after solid skin formation, heat transfer coefficient decreases sharply.

RESULTS AND CONCLUSION

Temperature distribution in terms of time and position as well as the color counters are the output of the computer simulation code.

Figures 8a and 8b represents cast and mold temperature distribution after pouring. Figures 8c and 8d demonstrate temperature distribution after complete solidification with and without air gap and contact resistance consideration, respectively.

It is seen that without consideration of the interface effect, an error of 50% in solidification time is observed.

The effect of contact resistance and air gap on temperature variation with time at a fixed point can be seen in Figures 9a to 9d.

Figure 9a represents the temperature variation time, while considering the interface effect at the geometrical center (half of cylinder height on the line

of symmetry) in the process of solidification. Figure 9b illustrates the temperature versus time with and without the interface effect consideration. Figure 9c shows the experimental results and numerical findings of temperature versus time considering the interface effect. It is clear that the simulation results are in very good agreement with the experimental findings.

Experimental and numerical results with and without the interface effects are represented in Figure 9d.

It is obvious that the interface effect consideration has resulted in a solidification time and temperature distribution close to the experimental findings. It is also important to note that consideration of the interface effect reduces the solidification time by 50% (close to the experimental results) and modifies the temperature distribution in the system drastically. Ignoring contact resistance and air gap particularly in the metallic mold can result in predictions that are far from reality. It is possible to calculate and implement the variation of the air gap using the model represented in this paper (ZTE) during the solidification process via viscoelasto-plastic modeling [11].

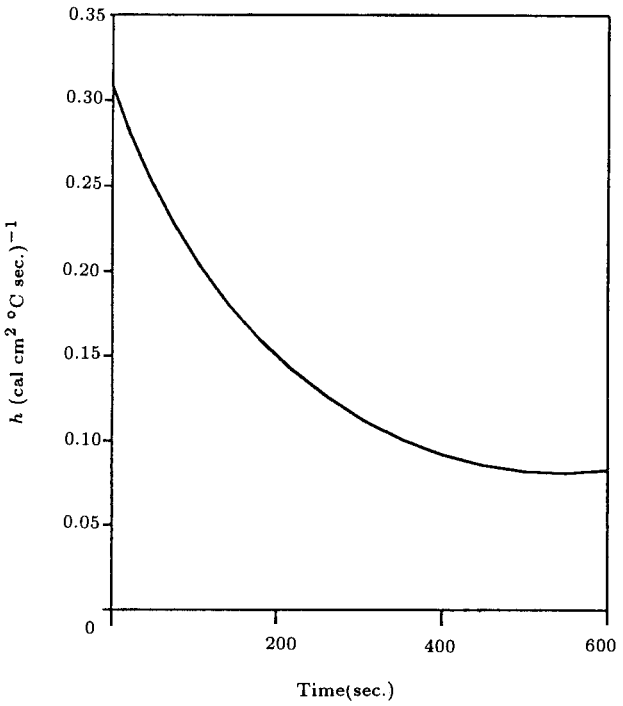

Figure 7. Overall heat transfer coefficient versus time at metal-mold interface.

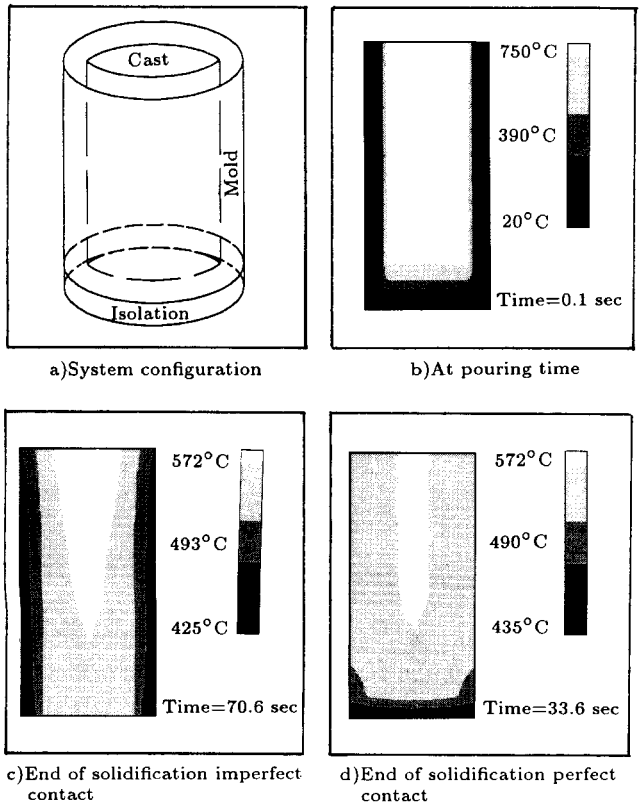

a)System configuration b)At pouring time

c)End of solidification imperfect contact d)End of solidification perfect contact

Figure 8. Temperature distribution in time and position.

NOMENCLATURE

β	temperature coefficient of thermal conductivity
Δt	time stepping scheme
Θ	weighting factor
λ	mean free path
μ	dynamic viscosity
ν	kinematic viscosity
A	interface area
c_p	specific heat at constant pressure
$[C]$	capacitance matrix
d	equivalent thickness of air gap
$\{F\}$	thermal load vector
Gr	Grashof number
h	overall heat transfer coefficient
h_b	heat transfer coefficient for boundary
k	thermal conductivity
k_g	gas thermal conductivity
$[K]$	conductivity matrix
Nu	Nusselt number
Pr	Prandtl number
q	heat flux through the interface
t	time
$\{T\}$	column matrix of all nodal temperature
T_a	ambient temperature
T_c	cast surface temperature
T_m	mold surface temperature

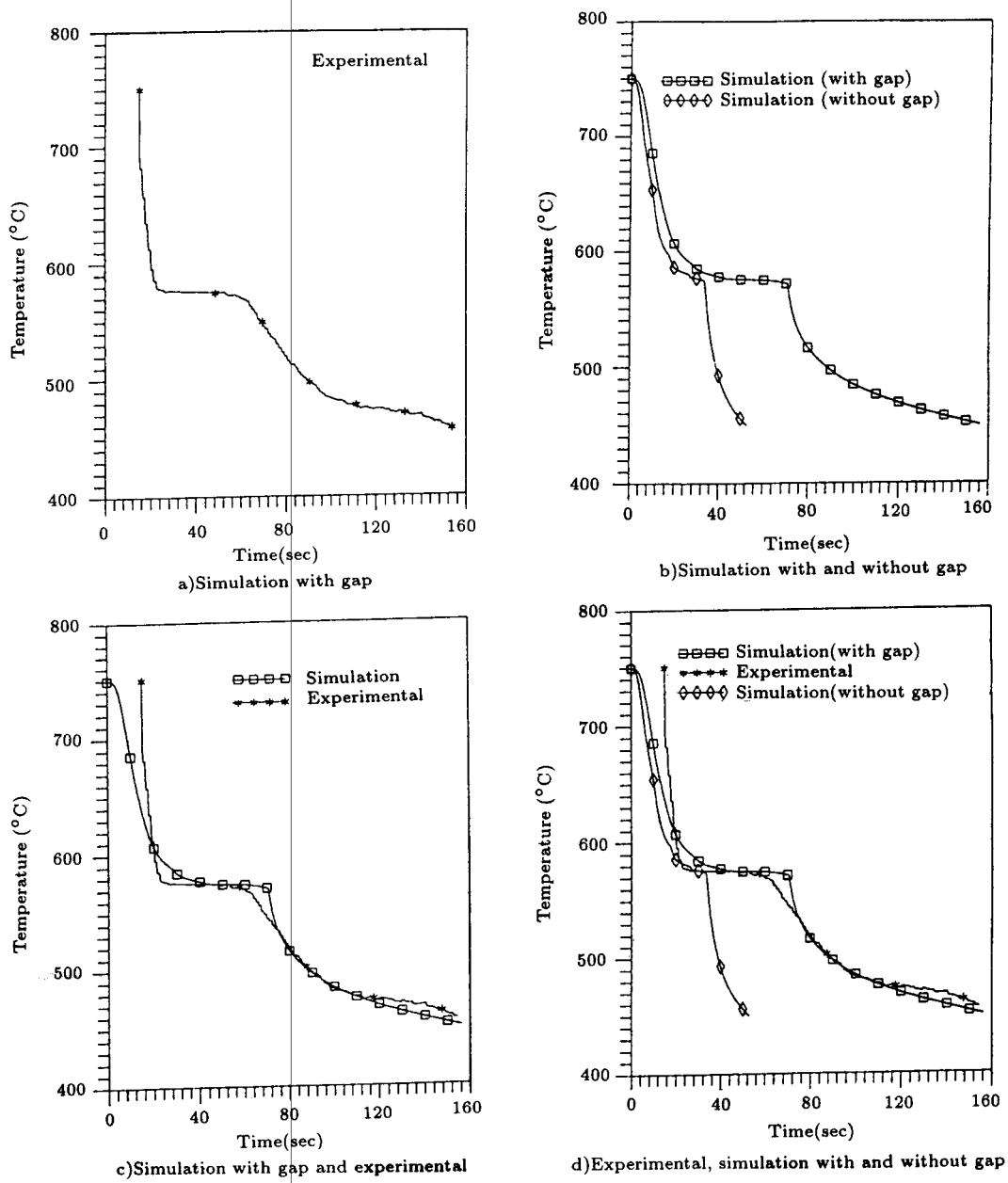

Figure 9. Variation of temperature at geometrical center with respect to time.

REFERENCES

1. Samonds, M., Lewis, R.W., Morgan, K. and Symberlist, R., *Computational Techniques in Heat Transfer*, **1**, Pineridge Press, Swansea (1985).
2. Tadayon, M.R. and Lewis, R.W., *Cast Metals*, **1**, p 24 (1988).
3. Isaac, J., Reddy, G.P. and Sharma, G.K., *AFS Transactions*, p 123 (1985).
4. Holman, J.P., *Heat Transfer*, McGraw-Hill Book Company, New York, USA (1981).
5. Song, S., Yovanovich, M.M. and Goodman, F.O., *J. of Heat Transfer*, **115**, p 533 (1993).
6. Sharma, D.G.R. and Krishnan, M., *AFS Transactions*, **91**, p 429 (1991).
7. Morgan, K., Lewis, R.W. and Zienkiewicz, O.C., *Int. J. Num. Eng.*, **12**, p 1191 (1978).
8. Zienkiwicz, O.C., *The Finite Element Method*, 3rd Edition, McGraw-Hill Book Company (1977).
9. Stasa, F.L. *Applied Finite Element Analysis for Engineers*, CBS Publishing Japan Ltd. (1985).
10. Shirinparvar, M., Davami, P. and Ahmadian, M.T. *Proceeding of the Third Annual ISME Conference*, **2**, Tehran, Iran, p 1097 (1995).
11. Shirinparvar, M. et.al, *Simulation of Cast Solidification Considering Air Gap Formation by Coupling Heat Transfer and Stress-Strain Analysis Using FEM*, in Preparation.